Preferred Orientation of Halite in a "Salt Seismogram"

W. M. Schwerdtner[1]
University of Toronto
Toronto, Ontario

ABSTRACT

The orientation of 100 halite grains in a specimen from the Winnfield Salt Dome, Louisiana, was determined on the universal stage. The orientation pattern obtained is very similar to those for the Grand Saline Salt Dome, published by Clabaugh.

A dynamic analysis of the fabric was made by assuming that the salt rock behaved like a rheid during doming. The orientation pattern observed agrees with the hypothetical pattern predicted by Calnan and Clews' theory for preferred orientation due to intragranular gliding. Kamb's theory for syntectonic crystallization predicts a state of preferred orientation dissimilar to the observed fabric pattern.

It is thus concluded that the present state of preferred orientation in the "salt seismogram" is mainly due to intragranular rotations and that crystallization during or after annealing did not markedly change the deformation pattern.

INTRODUCTION

It is generally believed that the flow of rock salt in domal structures does not exceed a few millimeters per year. Such low strain rates fall within the domain of creep. Although we have a fair knowledge on the creep properties of rock salt (Odé, 1962), virtually nothing has been published on the mechanics of creep.

Intracrystalline gliding and microfracturing seem to dominate primary creep of metamorphic rocks (Turner and Weiss, 1963, p. 314), whereas intergranular movements, grain boundary adjustments by local recrystallization, diffusion processes, and some translation gliding prevail during secondary creep.

During the rise of salt masses in the cores of domes, the halite grains are believed to undergo translation gliding, strain hardening, and subsequent annealing recrystallization. This mechanism has first been proposed by Leonhardt (1935) and Balk (1949). After the annealing is completed the halite grains are considered to deform again plastically. It should be mentioned, however, that such processes are probably restricted to the upper levels of the domes, where the temperatures are too low for diffusion to be the dominating mechanism of creep.

The Leonhardt school in Kiel, Germany, has done a number of experiments which show that under severe stress conditions halite aggregates will deform plastically and recrystallization,

---

[1]Department of Geological Sciences, University of Toronto, Toronto, Ontario. The work was carried out at the Department of Geological Sciences, University of Saskatchewan, Saskatoon, Saskatchewan. Thanks are due to Mr. George Golcak, University of Saskatchewan, for critically reading the manuscript, and the Saskatchewan Department of Mineral Resources, Records Branch, for making the drawings. The sample of the "salt seismogram" was taken during the Conference on Saline Deposits, 1962, with kind permission of the management of the Carey Salt Mine.

indicated by the loss of preferred orientation, takes place on subsequent heating (Gross, 1924; Leonhardt, 1937; Golusda, 1939). There is also evidence that deformed rock salt may anneal slowly at room temperature (Shlichta, 1962).

It is possible that, after slight strains, only mosaic recrystallization occurs within each grain but that the general crystal orientation is maintained (Shlichta, 1962). Moreover, it is well known that the deformation patterns of many cold worked metals remain virtually unchanged by annealing (Barrett, 1952, pp. 486 and 508).

Finally, under conditions of tectonic deformation involving low strain rates halite may recrystallize syntectonically (Turner and Weiss, 1963, p. 325). Such syndeformational crystallization has been observed in laboratory experiments with marble (Turner and Weiss, 1963, p. 353).

It thus appears that a given preferred orientation of halite in a salt dome could be due to mechanical orientation processes (translation gliding and grain rotation), annealing recrystallization, syntectonic crystallization, or else a combination of these processes.

In the absence of published fabric studies on rock salt deformed at low strain rates in the laboratory, the halite fabrics predicted by (i) Kamb's theory and (ii) Calnan and Clews' theory will be compared with the halite fabric obtained in a "salt seismogram" from Winnfield Salt Dome, Louisiana. Such a comparison can only be of value if the distribution of stress and strain during the formation of the "salt seismogram" can be successfully reconstructed.

SALT SEISMOGRAMS

This purely descriptive term has been introduced by Hartwig (1923) who distinguished several types of "salt seismograms" in the German salt stocks. The term seismogram was used to describe the appearance of deformed dark stringers in white salt. Balk (1949, p. 1806) misinterpreted Hartwig's writing and criticized the above expression substituting it by the term "shear folds." In the following discussions, the latter term is avoided as it already includes a genetic interpretation.

Salt seismograms are well known from many salt domes (Balk, 1949, Figs. 8-15; Hoy, Foose and O'Neill, 1962, Fig. 9). In the Gulf Coast domes, they appear to be confined to larger folds, but this is not generally true in the German salt stocks. Hartwig (1923, p. 195, Fig. 54) observed isolated seismograms on mine walls as well as on the roofs. He also noted that the salt of the seismograms was commonly extremely brittle in comparison with the rock salt in the adjacent areas (Hartwig, 1923, p. 194).

Some of the dark stringers (German: Linien) contain only 0.5 to 3 per cent more "insoluble material" than the light-coloured surrounding salt (Schwerdtner, 1962, table on page 267, sample no. 18-26). This suggests only small differences in competency. Hartwig (1923, p. 196) shows values of less than 10 per cent insoluble material. The values for the salt seismograms lie very close to those obtained for the straight stringers.

Let us now discuss the possible origin of the "salt seismograms." Balk's interpretation (1949, p. 1806) assumes differential slip on numerous surfaces parallel to the axial planes of the "shear folds." However, some authors are sceptical with regard to "pure shear folding" (Ramberg, 1963a, Fig. 9) and question such a mechanism for folding.

The formation of buckling folds or true drag folds (Ramberg, 1963b) requires rock layers with different competencies or anisotropic rocks that shear most easily in a direction quasi-parallel to the direction of compression (Ramberg, 1963a, p. 1). Such can probably be excluded for those salt strata which have diffuse and thin dark stringers that commonly appear very discontinuous under the microscope.

All "salt seismograms" drawn by Hartwig (1923) resemble rheid folds (Carey, 1953) involving nonuniform laminar flow parallel to the fold axes. This would imply quasi-continuous differential displacements along the axial planes. Carey uses a model of "two-dimensional" laminar flow (Mises, 1959, p. 24), where all the flow phenomena can be described in one plane normal to the flow laminae. The formation of small folds parallel to the direction of flow requires a shortening subparallel to the vertical layering which implies a convergence of the flow lines (Carey, 1953, Fig. 15; 1962, p. 128). If a model of three-dimensional nonuniform laminar flow is used

small folds or wrinkles parallel to the over-all direction of flow can be produced without convergence of the flow laminae.

DESCRIPTION OF THE ANALYZED SPECIMEN

An approximately oriented hand specimen (Fig. 1) was taken from a mine wall in the Carey Salt Mine, Winnfield Salt Dome, Louisiana. The specimen was cut from the central crest of a "seismogram fold" similar to the one in Fig. 8 of the paper by Hoy, Foose, and O'Neill (1962, Fig. 8).

The rock is composed of halite, small tectonic inclusions of white anhydrite (1-5 cm. long), and some diffuse dark stringers (Linien) of impure salt containing "clay material." Both the anhydrite and the dark stringers, which indicate the flow in the halite rocks, were originally part of a bedded salt rock. While the dark stringers have a competency (equivalent viscosity) close to that of halite the competency of anhydrite is considerably higher as indicated by boudinage (Fig. 1).

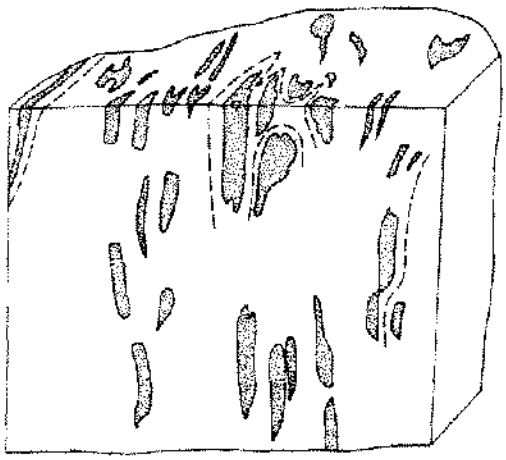

Figure 1. (3/4 x) Deformed layers of anhydrite (thickness exaggerated) from the crest of a "seismogram fold."

Some of the boudin-like inclusions may be "tear drops" (Carey, 1953, Fig. 20). Most common are relicts of tiny folds or fold closures (Rast, 1956, p. 402, Fig. 1b). Most tectonic inclusions are planar and lie approximately within one plane which is nearly vertical.

Some of the small rheid folds in the specimen are sufficiently outlined by dark stringers. In these cases, the approximate position of the fold axes can be obtained on suitable sections through the hand specimen. The brick-shaped anhydrite crystals within the white inclusions of anhydrite have a conspicuous preferred orientation of their long axes. Both the fold axes and the maximum for the apparent long dimensions of the anhydrite grains have a plunge of about 70 degrees.

METHOD OF ANALYSIS

The lattice orientations of 100 halite grains in thin sections parallel to the axial planes of the small folds were obtained on the universal stage. Every thin section was photographed and the grain boundaries, which could not readily be identified, were determined on the universal stage, and traced on the photographs. After the grain boundaries were known, the crystallographic orientations of the grains were obtained by successively setting two cleavage planes of each grain vertical on the universal stage. In this position, a cleavage trace has its minimum width.

The apparent long dimensions of the halite grains can be readily obtained on the photographs. Only those grains whose cleavages are approximately parallel to the thin sections may exhibit their true dimensions.

Most of the thin sections show little anhydrite as they were selectively cut from clean rock salt portions within the salt seismogram. In isolated groups of anhydrite grains, no preferred orientation of the grains is apparent.

ANALYTICAL RESULTS

The (100) planes tend to parallel the axial planes of the small rheid folds and the [100] directions tend to align with the direction of flow (fold axes). There are two incomplete girdles parallel and normal to the fold axes (Fig. 3). The former girdle has a greater point density.

Although heterogeneities in the fabric blur the minima, four areas of minimum density can be distinguished, which separate the two girdles. The minimum in the upper left-hand corner is least defined, but the trend is apparent from the concentration of the small minima.

The long dimensions of the apparent grain shapes (Figs. 2a, 2b) tend to form a maximum parallel to the fold axes.

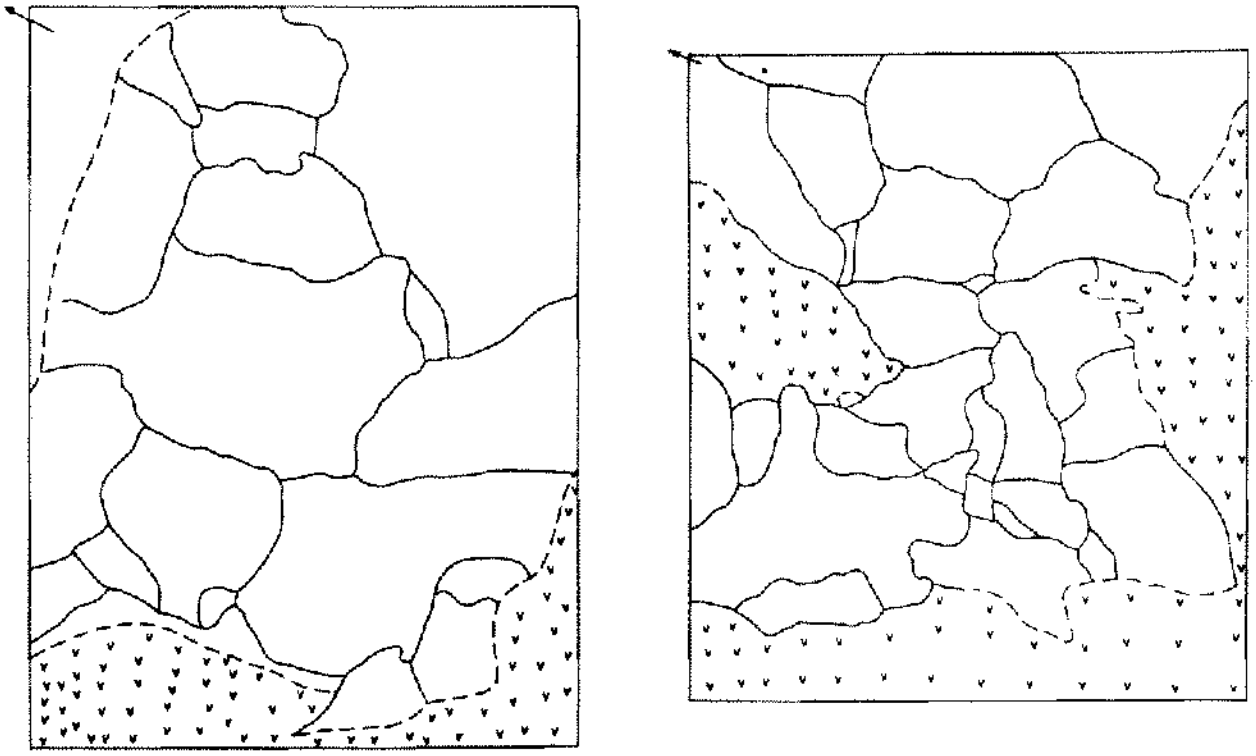

Figure 2. (3.6 x) Thin sections parallel to axial planes of folds in Figure 1. Arrows indicate plunge of fold axes; v = anhydrite.

DYNAMIC INTERPRETATION

It has been suggested above that "salt seismograms" are the result of rheid flow in quasi-isotropic salt rocks. Scheidegger (1963, p. 324) has pointed out that the actual rheological behaviour of rheids need not be specified, and that rheids can behave as plastic, elastoviscous or plasticoviscous bodies. The rheid flow of ice, which might be considered as the best known rheid, can be adequately described by the theory of plasticity, whereas the theory of viscous fluids fails to predict the change of flow rate in glaciers (Kamb, 1964, p. 355).

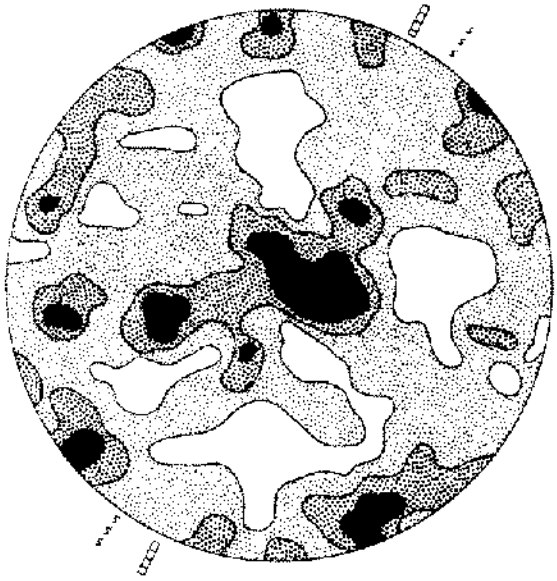

Figure 3. Preferred orientation of halite with respect to fold axes (~ ~) and lineation of anhydrite (□□□). 300 Poles of ((100)). ≥ 3 - 2 - 1 - 0.

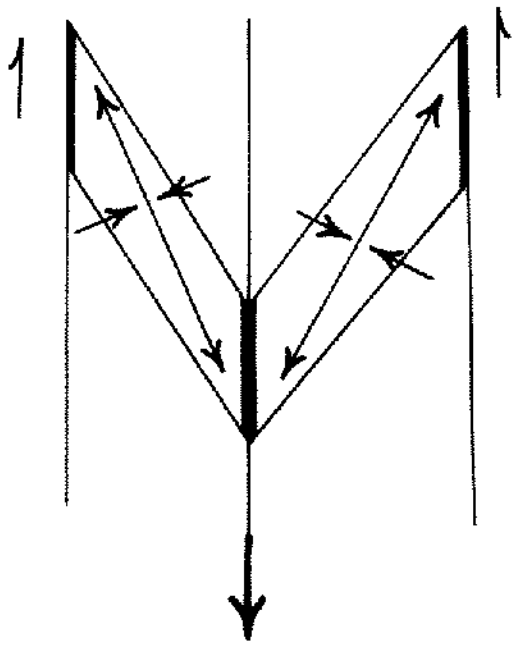

Figure 4. Laminar shear in two-dimensional flow. Diagonal of rhomboid is direction of maximum extension.

Let us now consider the strain distribution in the present "salt seismogram." We are only interested in the distortion of the rock and hence will disregard the large translation which is typical for rheid flow (Carey, 1962, Figs. 1, 19).

The behaviour of competent layers in a homogeneously strained incompetent matrix has been studied both theoretically and experimentally (Ramberg, 1959). The present "salt seismogram" presents such a case, where the total distortion of the incompetent rock salt is revealed by the deformation of the competent anhydrite layers (Fig. 1).

The remnants of the small folds of anhydrite clearly indicate buckling (Ramberg, 1959; 1963a), which should be expected as a result of the great difference in competency. Boudinage (Ramberg, 1955; 1959) occurred along the axial planes of the folds in vertical as well as in horizontal directions indicating two-dimensional extension. The parallel limbs of the tight folds (Fig. 1) have been rotated during buckling from a region of compression into a region of extension in the strain ellipsoid (Ramberg, 1959, p. 119); 1963a, p. 3). It is irrelevant whether there was boudinage or strong viscous shear resulting in the formation of "tear drops" (Carey, 1953, Fig. 20). Either process involves extension quasi-parallel to the axial planes (Fig. 4).

It can be assumed that the direction of maximum flow in the Winnfield Salt Dome was generally upwards (Hoy, Foose and O'Neill, 1962, p. 1454). The apparent maximum for the long dimensions of the anhydrite grains, which is an established indicator of the direction of maximum extension (Schwerdtner, 1964) was found, in the present hand specimen, to plunge fairly steeply. This implies a differential extension along the axial planes of the small folds (Fig. 1).

It is important to reconstruct the over-all strain distribution in the final phases of deformation, during which the present halite fabric might have been formed. There is no indication of extension normal to the axial planes which would have partially unrolled or stretched the tight relicts of the anhydrite folds (Fig. 1). Similarly, a horizontal compression parallel to the axial planes would probably have buckled the thin "tabulae" of anhydrite. Large differential displacements, parallel to the axial planes, would have rotated the planar inclusions of anhydrite (Fig. 1). Since the maximum extension is approximately vertical, we have a nonuniform tensile strain parallel to the axial planes of the folds and a compressive strain normal to the fold axes.

In order to apply the theories by Kamb (1959) and Calnan and Clews (1950, 1951), the approximate directions of principal stress acting on every halite crystal in the "salt seismogram" must be known. This cannot be readily achieved by applying the principles of continuum mechanics to the present salt rock, because the grains are relatively large with respect to the total structure. In particular, the paths of movement of small particles of material will not coincide with the smoothly curved flow lines in a homogeneously strained continuum (Ramberg, 1959, Figs. 1 and 9).

Calnan and Clews' theory was designed to analyze the deformation textures in specimens of polycrystalline metal. The directions of the external forces acting on such a specimen are generally known, and it is postulated that the external stresses are homogeneously propagated through the total specimen, in the initial phase of elastic deformation. After slight elastic strains, the principal stresses acting on the single grains will tend to become oblique to the external stresses and hence their directions are no longer controlled by the external stresses. However, the theory predicts these directions of internal stress, and an empirical approach yields the stable end positions of the grains with respect to the external stresses acting on the polycrystalline aggregate.

When applying Calnan and Clews' theory to the present "salt seismogram," we have to express its final deformation in terms of external forces acting on the specimen (Fig. 1). Although the over-all strain is probably caused by compressive stresses of different magnitudes, it may also be due to tensile stresses parallel to the directions of extension.

To avoid ambiguity, we resolve the unknown general state of stress into a hydrostatic part and a deviator (Turner and Weiss, 1963, p. 261). The total extension normal to the fold axes is considerably smaller than that parallel to it. If the former one is disregarded, the intermediate principal deviator stress is zero. The application of Calnan and Clews' theory is greatly facilitated by this simplification without changing the symmetry of the deviator.

The shearing stress which gives rise to the final distortion of the "salt seismogram" is now the result of a compressive stress normal to the axial planes and a tensile stress parallel to the fold axes. This concept is similar to the "plane parallelepipedal" deformation of Wever and Schmid (1930, p. 137).

Kamb's theory predicts statistically the most stable crystal orientations with respect to the directions of principal stress for the majority of the grains. The solutions derived from the application of continuum mechanics thus appear to be sufficiently accurate.

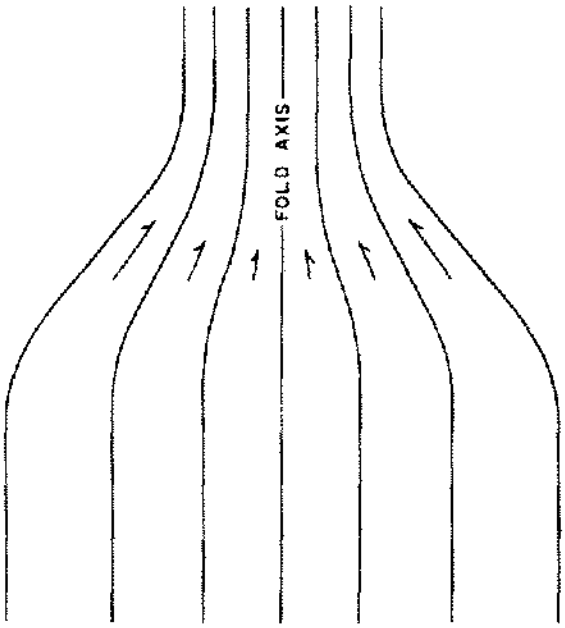

Figure 5. Converging flow lines during laminar flow. Arrows indicate direction and assumed magnitude of flow.

In our model of "two-dimensional" rheid flow with converging flow laminae (Fig. 5), there is only an undimensional extension. In order to account for the two-dimensional extension in the present "salt seismogram" we have to assume diverging flow lines within every lamina, which gives rise to diverging fold axes.

Although there is neither a conspicuous convergence of the flow laminae nor a conspicuous divergence of the fold axes in the present hand specimen, they might be apparent on a larger scale. The total extension normal to the fold axes would be relatively small assuming that the salt rock was incompressible and that the major extension occurred parallel to the fold axes.

Although it is impossible to outline the stress distribution in an isotropic continuum without specifying its rheologic behavior, the orientation of the principal plane parallel to the extreme stresses follows from the assumption of plane deformation. Even in the viscous case, the directions of maximum and minimum principal stress form angles

of 45 degrees with the flow laminae, and exchange their positions with changing sense of laminar shear. Converging flow laminae give rise to a gradual shifting of the principal directions with respect to the axial planes of the anhydrite folds (Fig. 5).

A reconstruction of the principal planes is sufficient for the present application of Kamb's theory. The plane of maximum and minimum principal stress is perpendicular to the axial planes of the small folds (front surface of the specimen in Fig. 1).

Let us now consider the applicability of Kamb's thermodynamic theory of competitive crystal growth to the syntectonic recrystallization of tectonites. The theory assumes that every grain is stressed below the elastic limit, while grain boundary migration and diffusion give rise to drastic changes of the grain shapes. The rock as a whole may thus undergo a finite strain.

Recently, Kamb (1962) has demonstrated in experiments with ice the validity of his thermodynamic theory. Syntectonic crystallization has been observed in extension tests with dry marble (Griggs, Turner and Heard, 1960, pp. 94-97). Intergranular as well as intragranular recrystallization occurred in the highly strained fabrics. The c-crystallographic axes of the growing grains tend to be normal to the unique axis of stress as predicted by Kamb (1959, p. 166), although most of the original grains appear to have been stressed beyond the elastic limit.

Kamb's theory applied to the present "salt seismogram" predicts a state of preferred orientation dissimilar to the observed orientation pattern (Fig. 3). The theory does not predict a pronounced girdle in the plane of the greatest and least principal stresses, as was shown by Clark and Schwerdtner (paper in this symposium). Moreover, the pronounced maxima in this girdle should not form angles of 45 degrees.

Geologists may learn much about the internal deformation processes in rocks by analogy with the better known relationships in polycrystalline metals. Metallurgists have studied the lattice rotation of single crystals in uniaxial tension and compression tests (Taylor and Elam, 1925; Taylor, 1927). General rules as to the behaviour of single crystals were derived (Barrett, 1952, p. 371).

In tension tests, translation gliding along one slip system (single slip) moves the glide direction towards the axis of tension until gliding along a second slip system starts. During subsequent duplex slip, the lattice rotates in such a way that the shear stresses at the two active slip systems remain equal. The stable end position is reached when the two glide directions and the axis of tension as bisectrix lie in one plane.

In compression tests the normal to the active glide plane moves towards the compression axis until duplex slip starts. The stable end position is reached when the two poles of the active slip planes and the compression axis as bisectrix lie in one plane.

The behaviour of the individual crystals in polycrystalline aggregates is the subject of a number of theories which predict the stable end positions in uniaxial tension and compression tests. Both deformation processes can be superimposed to obtain a "plane parallelepipedal deformation" (Wever and Schmid, 1930) which is similar to the final deformation of the "salt seismogram."

At room temperature, halite glides along (110) and (100). It is uncertain whether slip along (111) occurs at room temperature, but gliding along this plane has been observed at 100 degrees centigrade (Taumann and Salge, 1928). The direction of slip in halite is always $[[110]]$.

The critical resolved shear stresses (τ_c) for halite at room temperature were determined by Dommerich (1934).

$\tau_{110} = 76.4 \pm 3.5$ gms/mm^2

$\tau_{111} = 187 \pm 8$ gms/mm^2

$\tau_{100} = 238 \pm 10.6$ gms/mm^2

The present sample was taken at a depth of 811 feet. It can be assumed that the temperatures during the late stages of deformation of the "salt seismogram" were somewhat higher than

room temperature. However, the ratio of the critical resolved shear stresses $\tau_{110}:\tau_{111}:\tau_{100}$ at 400 degrees C is close to that at 20 degrees centigrade (Wolff, 1935, p. 162). It should be noted that only the ratios of the critical shear stresses appear in the mathematical expressions below.

It is well known that translation gliding can occur during creep when the applied shear stress remains below the critical resolved shear stress values (Azaroff, 1960, p. 137). Furthermore, Smekal (1935) and his collaborators emphasized that a critical resolved shear stress indicates the point of detectable slip rather than the beginning of intracrystalline gliding. However, it is likely that halite when nonrecoverably strained always slips most readily along ((110)) and least easily along ((100)).

Only a few theories for cold working of metal aggregates predict stable end positions of the individual grains and the mechanisms whereby these end positions are reached. While the theories by Taylor (1938) and Bishop (1954) assume that every grain is homogeneously deformed, Calnan and Clews' theory accounts for the behaviour of both homogeneously and inhomogeneously strained grains (1950, p. 1088).

Translation gliding in a grain can occur simultaneously along two slip systems (duplex slip) and along three or more systems (multiple slip). Intracrystalline rotations result from any of those except in the case of three or more slip systems symmetrically disposed about the direction of applied stress (Pickus and Mathewson, 1939, p. 246). Lattice rotations are conveniently represented by the rotation of the direction of applied stress over the unit triangle (Fig. 6). The critical resolved shear stresses must be attained on two or more slip systems at the same time in order to guarantee ruptureless deformation in a polycrystalline aggregate. If a grain deforms by duplex slip the effective stress may be represented by a tensile stress Te.

There is at least one favourable slip system for a given grain of any position within the unit triangle (Fig. 6). For this slip system $\cos\chi\cos\lambda$ is a maximum. χ is the angle between the direction of applied stress and the normal of the most favourable slip plane, whereas λ is the angle between the direction of applied stress and the direction of slip. As the three critical resolved shear stress values for halite are different ($\tau_{110} < \tau_{111} < \tau_{100}$) corresponding factors have to be added to account for these differences (Calnan and Clews, 1951, p. 624).

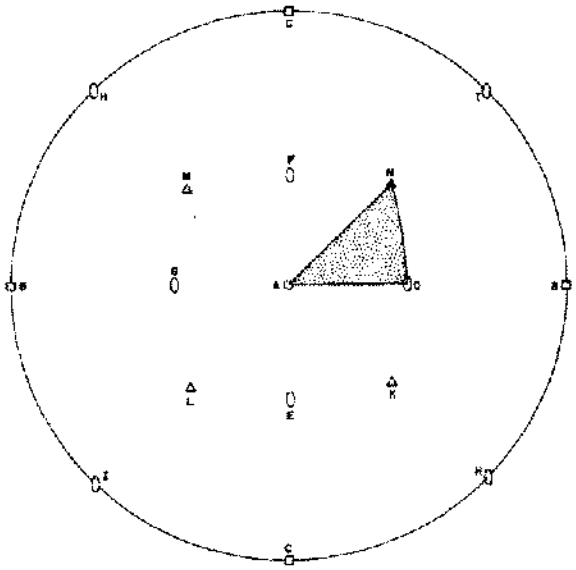

Figure 6. Cubic directions (□ = four-fold axes, Δ = three-fold axes, ○ = two-fold axes) and unit triangle ADN.

Let us now consider a grain of known orientation with respect to the applied stress Ta (Calnan and Clews, 1950). At the instant of application of a small stress, Te will coincide with Ta. On elastic deformation, intergranular stresses come into play which cause Te to move away from Ta. As the value of Ta rises the resolved shear stress rises proportionally until it teaches the critical value for slip.

Most grains in deformed metal aggregates do not undergo single slip as has been outlined above. It follows that Te must have moved away from the direction of applied stress such that Te resolved on the most favourable glide system is always lower than the critical resolved shear stress. If Te reaches an area of duplex slip in the unit triangle translation gliding may occur, or else Te may move into a position for multiple slip. If such a position corresponds with a minimum for $\cos\chi\cos\lambda$, Te has reached its final position as any further increase in Ta must result in translation gliding.

In case of three or more symmetrically disposed slip systems there is no grain rotation. Consequently, in order to obtain a high degree of preferred orientation, there must be a

considerable amount of single and duplex slip in an aggregate, although some multiple slip is necessary to retain cohesion at the grain boundaries (Calnan and Clews, 1951, p. 617).

To apply the above theory to the present deformation of halite two cases have to be considered as it is uncertain whether ((111)) is a slip plane at temperatures around 50 degrees centigrade. It will be shown, however, that it makes little difference whether halite glides along ((111) or not.

Table 1 shows the values of $\cos\chi\cos\lambda/\tau_c$ for the most favourable slip systems at 20 points of the unit triangle (Fig. 8). If $\frac{\cos\chi_1\cos\lambda_1}{\tau_{100}} > \frac{\cos\chi_2\cos\lambda_2}{\tau_{111}} \geq 0$, slip will first occur on (100), and hence (100) is the more favourable system. The above inequality can also be written as $\cos\chi_1\cos\lambda_1 > \frac{\tau_{100}}{\tau_{111}}\cos\chi_2\cos\lambda_2 \geq 0$. The ratios of the critical resolved shear stresses seem to be fairly independent of temperature. Hence the relationships derived below are generally valid for deformations at any temperature between 20 and 400 degrees centigrade.

Figure 7 shows that the values of $\cos\chi\cos\lambda/\tau_c$ for the most favourable slip systems decrease as Ta approaches [111] which is the minimum. There is also a general decrease toward the boundary DN of the unit triangle. Table 1 also lists the most favourable slip systems [Fig. 6] for each position of Ta.

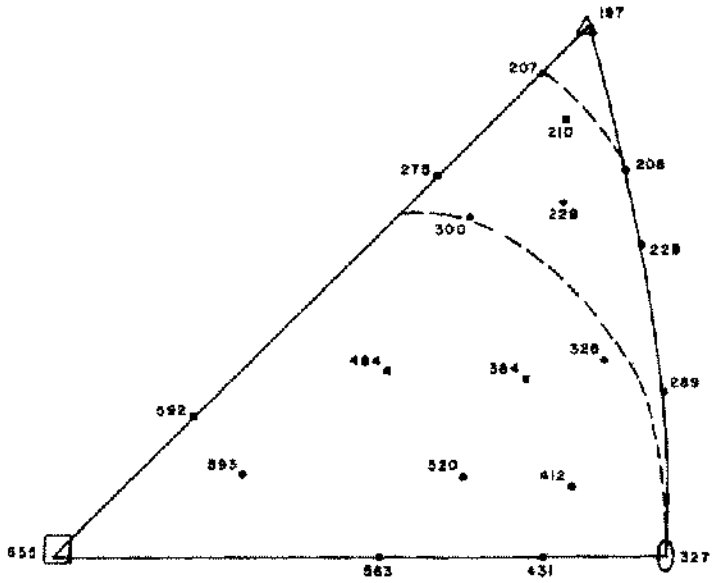

Figure 7. Unit triangle with relative shear stresses on the most favourably oriented slip planes. Values of $\frac{\cos\chi\cos\lambda}{\tau_c}\cdot 10^5$ were plotted.

It can be readily seen from Table 1 that single slip can only occur in the vicinity of P_5 and P_{14}. If single slip does not occur when Ta parallels P_5, Te will move normal to the dashed contour in Fig. 7 along the line of quickest descent to the triangle boundary, where duplex slip may start. However Te may reach N where subsequent translation gliding does not result in any lattice rotation.

The lattice rotations due to duplex or multiple slip, after Te has moved away from Ta, are shown by dashed arrows in Fig. 8 and Fig. 9. The lattice rotations for duplex slip and for asymmetrical multiple slip, before Te has moved away from Ta, under applied tension or compression, are indicated by solid arrows in Fig. 8 and Fig. 9.

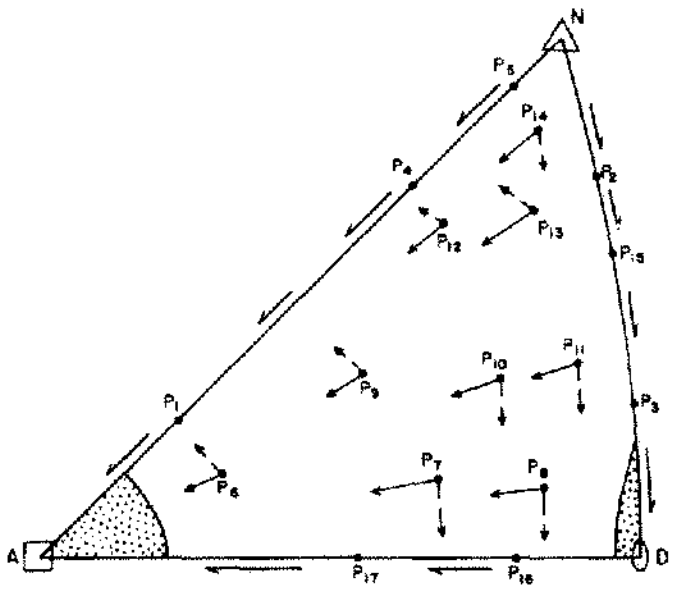

Figure 8. Lattice rotation in rock salt under uniaxial compression.

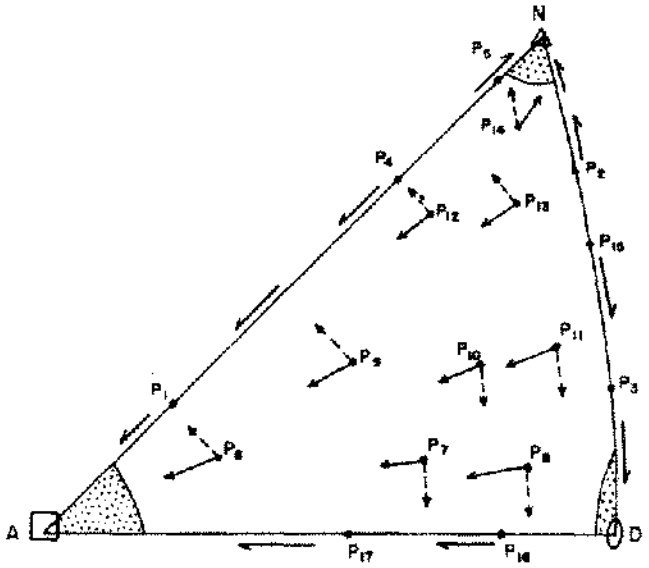

Figure 9. Lattice rotation in rock salt under uniaxial tension.

There is a line of multiple slip approximately parallel to the dashed contours in Figure 7, which runs between P_{13} and P_{14}. However, no point of symmetrical multiple slip exists as can be readily confirmed on the stereographic net.

Under uniaxial compression the only stable end positions are [100] and [110] where symmetric multiple slip occurs (Pickus and Mathewson, 1939, p. 246).

Dobson and Wilman (1961) conducted uniaxial compression tests with halite powders and applied Calnan and Clews' theory to explain their results ([100] parallel to the unique stress axis). It should be pointed out, however, that Calnan and Clews' theory applies to polycrystalline aggregates and not to powders, and that considerably intergranular rotations of the rectangular halite particles will have occurred in an early experimental stage, prior to the compaction of the powder.

Table 1

Position of T_c in unit triangle	Most favourable slip systems, each one defined by normal to slip plane and slip direction (Fig. 5)	$\frac{\cos\chi\cos\lambda}{\tau_c}$	Number of most favourable slip systems with equal $\frac{\cos\chi\cos\lambda}{\tau_c}$
A	FE, EF, GD, DG	0.00655	4
D	EF, FE, IH, HI	0.00327	4
N	AI, BF, CD	0.00197	3
P_1	EF, FE, DG, GD	0.00592	4
P_2	AI, BF | KF, KI	0.00204 | 0.00208	2 | 2
P_3	EF, FE, IH, HI	0.00289	4
P_4	DF, FD, EG, GE	0.00275	4
P_5	AI	0.00207	1
P_6	EF, FE	0.00593	2
P_7	EF, FE	0.00520	2
P_8	EF, FE	0.00412	2
P_9	EF, FE	0.00484	2
P_{10}	EF, FE	0.00384	2
P_{11}	EF, FE	0.00326	2
P_{12}	EF, FE	0.00300	2
P_{13}	EF, FE	0.00229	2
P_{14}	AI	0.00210	1
P_{15}	EF, FE, IH, HI	0.00228	4
P_{16}	EF, FE	0.00431	2
P_{17}	EF, FE	0.00563	2

Such processes are not considered in Calnan and Clews' theory (1950). Also, the previous application of the theory is incorrect as there is asymmetric multiple slip on the [110] - [111] boundary. It can be readily confirmed on the Wulff net that there is a resultant rotation when the four lattice rotations due to single slip are added. Consequently, there are two stable end positions, namely [100] and [110].

Under uniaxial tension, there are three stable end positions, [100], [110], and [111]. The latter maximum, however, has a low density, and a considerable scatter should occur around [111] as both Ta and Te move towards it (Calnan and Clews, 1950, p. 1092).

If ((111)) is considered as a third slip plane, only the situation in P_2 changes (Table 1). No changes occur in Fig. 8 or Fig. 9.

Following Calnan and Clews' procedure (1950, p. 1095), the ways in which both tension and compression end positions may be satisfied simultaneously shall be examined. The superposition of both deformation processes is to simulate the final distortion of the "salt seismogram."

The uniaxial compression normal to the axial planes of the small folds produces a fabric in which, for most crystals, the direction of compression will lie close to [100] and [110], the latter being the weaker maximum.

Let us assume that Ta in the crystals either parallels [100] or [110]. Since the direction of flow is perpendicular to the uniaxial compression, the direction of flow must lie on the great circles (100) and (110) in Fig. 10. At the same time uniaxial tension parallel to the over-all direction of flow will tend to produce maxima according to those in Fig. 9.

The only direction which completely satisfies both a tension and the major compression end positions is [100]. This determines the strongest maximum within the (100) plane in Fig. 10. As a result the hypothetical fabric pattern (Fig. 11) is dominated by maxima for [[100] within the axial plane, parallel and normal to the direction of flow, as well as a maximum for [[100]] normal

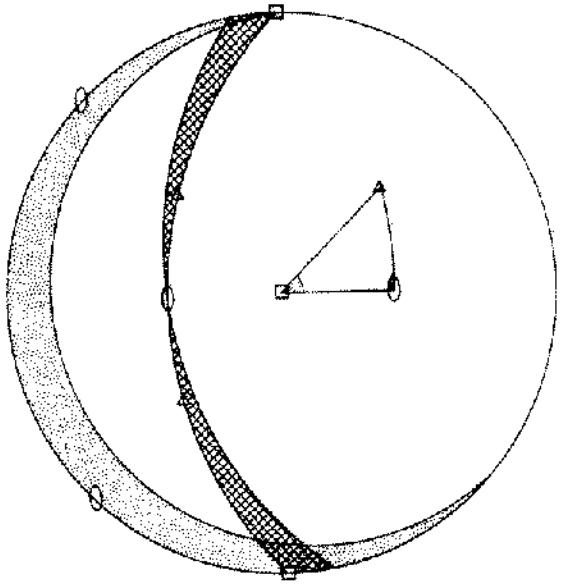

Figure 10. Superposition of tension and compression; shaded areas contain the great circles for all poles within the maxima of the unit triangle.

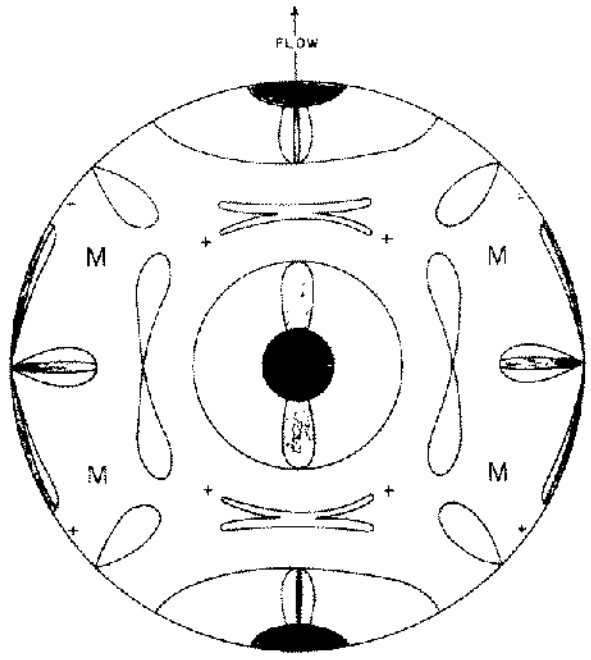

Figure 11. Hypothetical fabric pattern for rock salt; construction according to Mellis (1954). Crosses indicate centres of areas with minor density due to the weak maximum around [111] in Figure 9. M designates areas of minimum density.

to the axial plane. There is also a weak maximum for [[100] parallel to the direction of flow when ((110)) parallels the axial plane. The orientations of further sub-maxima are listed in Table 2. The planes listed are parallel to the axial planes of the small rheid folds of the salt seismogram whereas the directions listed coincide with the direction of flow.

Table 2

Direction of tension (direction of flow)	Direction of compression (normal to axial planes)	Resulting preferred orientation (lattice planes parallel to flow, laminae and lattice directions parallel to direction of flow)
[100]	[100] , [110]	[100] on (100) and (110)
[110]	[100] , [110]	[110] on (100) and (110)
[111]	[110]	[111] on (110)

The resulting hypothetical fabric is pictured in Fig. 11 where it is assumed that the scatter of poles is greater than the scatter in Fig. 8 and Fig. 9. It is clear that the [[111]] alignment with the direction of flow represents the weakest submaximum, as the point concentration around [111] in Fig. 9 is rather scattered itself. If the hypothetical fabric is compared with the observed orientation pattern [Fig. 3] good agreement is apparent. The preferred orientation of the long axes of the grains is in accordance to the postulated grain deformation.

CONCLUSIONS

The observed fabric in the salt seismogram can be fully explained on the basis of Calnan and Clews' theory whereas Kamb's theory does not adequately explain it. The present fabric resulted from translation gliding in the halite grains during the final phases of deformation and subsequent annealing crystallization did not notably alter the deformational fabric pattern. It is also possible that recovery from strain hardening proceeded without recrystallization as it takes place in cold worked metals heated up to moderately high temperatures (Turner and Weiss, 1963, p. 332) whereby the deformation fabric is retained.

Clabaugh (1962a) who measured the positions of the large grains in 6 samples from Grand Saline Salt Dome, Texas, obtained orientation patterns (1962b, Diags. B, C, D, E) which are very similar to the present pattern in Fig. 3. It is possible that Diags. A and F also represent the same fabric pattern provided the direction of "external compressive stress" was oblique to the axial "planes," or else that the position of the axial planes in Clabaugh's diagrams is somewhat inaccurate.

It thus appears that most of the fabric patterns obtained by petrofabric analysis of samples from Grand Saline Salt Dome and Winnfield Salt Dome reflect the plastic deformation of halite during salt flow. Many grains in the samples analyzed by Clabaugh (1962b, p. 9) were bent or warped which suggests that the fabrics may not have undergone complete recrystallization. However, few crystals in the present fabric are noticably bent, and no slip striae were observed under crossed nicols.

REFERENCES

Azaroff, L. V., 1960, Introduction to solids: McGraw-Hill Book Company, New York.

Balk, R., 1949, Structure of Grand Saline Salt Dome, van Zandt County, Texas: Am. Assoc. Petroleum Geologists Bull., vol. 33, pp. 1791-1829.

Barrett, C.S., 1952, Structure of metals: McGraw-Hill Book Company, New York.

Bishop, J.F.W., 1955: Mech. Phys. Solids Jour., vol. 3, pp. 130-142, pp. 259-266.

Calnan, E.A., and Clews, C.J.B., 1950, Deformation textures in face centered cubic metals: Philos. Mag., vol. 41, pp. 1085-1100.

_____, 1951, Development of deformation textures in metals, part 2: Philos. Mag., vol. 42, pp. 616-635.

Carey, S.W., 1953, Rheid concept in geotectonics: Geol. Soc. Australia Jour., vol. 1, pp. 67-117.

_____, 1962, Folding: Alberta Soc. Petroleum Geologists Jour., vol. 10, pp. 95-144.

Clabaugh, P.S., 1962a, Petrofabric study of deformed salt: Science, vol. 136, pp. 389-391.

_____, 1962b, Petrofabric analysis of salt crystals from Grand Saline Salt Dome: M. Sc. Thesis, University of Texas.

Dobson, P.S., and Wilman, H., 1961, Compression textures of polycrystalline materials of rock salt type: Acta Crystallographica, vol. 14, pp. 1275, 1277.

Dommerich, S., 1934, Festigkeitseigenschaften bewaesserter Salzkristalle, 4. Richtungsabhaengigkeit der Streckgrenze geleichmaeszig abgeloester Steinsalzstaebschen: Zeitschr. f. Physik, vol. 90, p. 189.

Golusda, G., 1939, Zur Rekristallisationsfrage in der Petrographie nebst einem experimentellen Beitrag zur Rekristallisation von Steinsalz, Sylvin und Anhydrit: Schriften aus dem Mineralogisch-Petrographischen Institut der Universitaet Kiel, Heft 7.

Griggs, D.T., Turner, F.J., and Heard, H.C., 1960, Deformation of rocks at 500 to 800 degrees centigrade: Geol. Soc. America Mem. 79.

Gross, R., 1924, Verfestigung und Rekristallisation: Zeitschr. Metallkunde, vol. 16, p. 344.

Hartwig, F., 1923, "Salz-Seismogramme," ihre tektonische und praktische Bedeutung: Kali, vol. 17, pp. 193-197.

Hoy, R.B., Foose, R.M., and O'Neill, B.J., 1962, Structure of Winnfield Salt Dome, Winn Parish, Louisiana: Am. Assoc. Petroleum Geologists Bull., vol. 46, pp. 1444-1459.

Kamb, W.B., Theory of preferred crystal orientation developed by crystallization under stress: Jour. Geology, vol. 67, pp. 153-170.

_____, 1962, Experimental test of theories of nonhydrostatic thermodynamics: Jour. Geophys. Research, vol. 67, p. 1642.

_____, 1964, Glacier geophysics: Science, vol. 146, no. 3642, pp. 353-365.

Leonhardt, J., 1935, Neue Beobachtungen and Ausschauungen ueber Salzmetamorphose and Salztektonik: Fortschr. d. Mineralogie, vol. 19, p. 37.

_____, 1937, Gefuege und Umformung von Salzmassen mit Bezug auf Vorgaenge, die an den festen Zustand gebunden sind: Kali, vol. 31, pp. 81-86, pp. 91-94, pp. 101-103.

Mellis, O., 1954, Einiges zur Geometrie der Lagekugelbesetzung: Tschermaks Minerlog. Petrogr. Mitt., vol. 4, pp. 138-144.

Mises, R. von, 1959, Theory of flight: Dover Publications, New York.

Odé, H., 1962, International Conference on Saline Deposits, Program, p. 27.

Pickus, M.R., and Mathewson, C.H., 1939, Theory of the origin of rolling textures in face centred cubic metals: Inst. of Metals Jour., vol. 64, pp. 237-260.

Ramberg, H., 1955, Natural and experimental boudinage and pinch-and-swell structures: Jour. Geology, vol. 63, p. 527.

Ramberg, H., 1955, Evolution of ptygmatic folding: Norsk Geol. Tidsskr., vol. 39, pp. 99-151.

_____, 1963a, Strain distribution and geometry of folds: Geol. Inst. University of Uppsala Bull., vol. XLII.

_____, 1963b, Evolution of drag folds: Geol. Mag., vol. 100, pp. 97-106.

Rast, N., 1956, Origin and significance of boudinage: Geol. Mag., vol. 93, pp. 401-408.

Scheidegger, A. E., 1963, Principles of geodynamics: Academic Press Inc., New York.

Schwerdtner, W. M., 1962, Untersuchungen an bunten Augensalzen der Ronnenberg-Gruppe (Zechstein 3) von Hannover: Kali and Steinsalz, vol. 3, pp. 265-274.

_____, 1964, Gefuegestudien an Anhydritbaenken im Benther Salzstock (Werk Ronnenberg): Kali und Steinsalz, vol. 4, pp. 64-70.

Shlichta, P., 1962, in Ode, H., Resume of work session, International Conference on Saline Deposits (Unpublished).

Smekal, A., 1935, Eine neue Translationsbedingung: Zeitschr. f. Physik, vol. 93, p. 171.

Taumann, G., and Salge, W., 1928: Neues Jahrbuch f. Mineral. und Pal., Beil. Bd. 57, p. 117.

Taylor, G.I., 1927, Distortion of crystals of aluminum under compression, part 2: Roy. Soc. (London) Proc., vol. A116, pp. 16-39.

_____, 1938, Stephen Timoshenko 60th Anniversary Volume, Macmillan, New York, p. 218.

Taylor, G.I., and Elam, C.F., 1925, Plastic extension and fracture of aluminum crystals: Roy. Soc. (London) Proc., vol. A108, pp. 28-51.

Turner, F.J., Weiss, L.E., 1963, Structural analysis of metamorphic tectonites: McGraw-Hill Book Company, New York.

Wever, F., and Schmid, W.E., 1930, Texturen kaltverformter Metalle: Zeitschr. f. Metallkunde, vol. 22, pp. 133-140.

Wolff, H., 1935, Richtungsabhaengigkeit des Translationsmechanismus von Steinsalzkristallen in hoeheren Temperaturen: Zeitschr. f. Physik, vol. 93, pp. 159-169.